COLD COMPRESSION OF CYLINDRICAL, TAPERED AND FLANGED SPECIMENS

Mohieldeen Abdel-Rahman and Bashir Raddad

Mechanical and Industrial Engineering Department
El-Fateh University, Tripoli, LIBYA, P. O. Box 13276 Tripoli
e-mail: drmohie@yahoo.com

الملخص

في اختبار الضغط للعينات المخروطية و تلك ذات الحلقة في المنتصف، يمكن الحصول على حالات إجهاد في مناطق الانفعالات الصغيرة لمسار الكسر في هذا الاختبار الهام. في هذا العمل، تم استعمال عينات غير تقليدية بجانب العينات التقليدية (الأسطوانية) من 3 مواد مختلفة (صلب منخفض الكربون ، سبيكة ألومنيوم تحوى 4% نحاس و نحاس أصفر) و قد تم تصميم التجارب بحيث تعطى مجالاً واسعاً لتغير الأبعاد بالنسبة للعينات المختلفة. و قد تم دراسة تأثير نسبة الطول \ القطر الأصلية و النسب الهندسية الأخرى على منحنيات الإجهاد–الانفعال، و تم أيضا دراسة أنواع الكسور للأشكال المختلفة .

ABSTRACT

In this work, workability testing was performed through cold compression of flanged and tapered specimens along with the commonly-used cylindrical ones. Such specimens can give stress states in the small strain regions of the fracture locus. Three materials were used, low carbon steel, an Aluminum alloy containing 4% copper and brass. Typical stress/strain curves were presented for the different materials. Effect of the initial Ho/Do ratio and other dimensional factors were investigated. Surface fractures for the different specimen geometries were also detected**.**

KEY WORDS: Compression, Tapered and flanged specimens, Fractures

INTRODUCTION

Workability; a term specified for use with ease of deformation in bulk forming processes; is a complex phenomenon which depends on both material properties and process parameters [1]. Depending on the stress state, two types of surface fracture are possible: internal and surface fractures, both are sensitive to micro structural-scale non homogenities and inherent isotropy [2-3]. Process parameters include: maximum strain achieved, temperature, strain rate and interface friction. Metalworking processes usually produce different states of stresses. Severity of stress system with regard of workability increases with the level of tensile stresses. For a given material, at certain temperature and strain rate, workability is much greater for a more compressive stress state. Even in a process that is predominately compressive in nature, local tensile stress can arise. These stresses, often called secondary tensile stresses, become primary (in importance) in determining workability of metals [4-6].

Axial compression of cylinders provides a deformation test in which the average stress state is inherently similar to that in bulk forming processes. Scribed grid marks are applied to the specimen surface and the specimen is incrementally compressed under certain conditions until cracks on the bulged surface are observed. For each incremental

deformation, displacement is measured and maximum diameter is measured. Axial and circumferential strains on the equatorial surface are then calculated using the following equations:

$$\text{Axial strain } (\varepsilon_z) = \ell n\left(\frac{h}{h_o}\right) \quad (1)$$

and

$$\text{Circumferential strain } (\varepsilon_\theta) = \ell n\left(\frac{w}{w_o}\right) \quad (2)$$

where; h and h_o are the initial and final grid height respectively and w and w_o are the initial and final grid width respectively. Fracture plane proved to coincide with the maximum shear stress plane. Fracture strain combinations followed a straight line according to Kudo and Aoi [7]. Kobayashi developed a tentative analysis for the relationship between barreling and strains at the free surface [8]. Fracture observations were the same as suggested in Ref. [7]. Kuhn and his co-workers extended this principle to the bolt heading process [9].

Fracture is an extremely complex phenomenon which depends on the microstructure of the material in combination with the stress and strain states during deformation. Void coalescence under shear deformation and local plastic instability play also a role in the ductile fracture in forming. Based on the localized deformation and instability, several theoretical models have been developed [7-16]. Each model provides essentially the material behavior in the large strain region (straight line slope of 0.5) but deviations may occur in the small strain region. The small strains cannot be achieved through conventional cylindrical specimens, so tapered and flanged shapes were used [17].

One method of producing strains in this region is to artificially pre bulge the test specimens by machining a taper or a flange on the cylinders. Then compression causes lateral spread of the inside material which expands the rim circumferentially with little or no axial compression being applied to the rim. Thus tapered and flanged upset test specimens provide strain states for measurement of the fracture strains when the compressive strains are small. Each combination of height-to-diameter and change in flange thickness leads to a different ratio of tensile to compressive strain during the test. The experimental results of compressing the tapered and flanged specimens proved to agree with the model of Marciniak-Kuczynski analysis for both the uni-slope and dual slope results. The behavior of such specimens in compression gives a typical straight line relationship like the cylindrical specimens in some materials, however, for other materials and in other range of temperatures and strain rates this principle does not apply. Although the compression of cylindrical specimens was detailed in many publications [7-8,13-15], details of such behavior varying geometrical parameters such as specimen height to diameter ratio, flange dimensions, tapered part geometry were rarely found in the literature.

This work focuses on the investigation of the workability testing of such specimens. For comparison, flanged and tapered specimens were used along with the commonly-used cylindrical ones.

EXPERIMENTAL WORK

Three test materials, low carbon steel, an aluminum alloy containing 4% copper and brass were used. Test specimens were machined according to the dimensions in Figures 1. Compression tests were conducted on a 100 ton Zwick universal testing machine

having a maximum axial displacement of 100 mm. Cross head speed was kept as 5 mm/minute for all experiments. The original diameter of all specimens was kept as 22 mm. This presents the original diameter of the cylindrical specimen, the flange diameter in the flanged specimen and the diameter of the cylindrical mid part in the tapered specimen. Specimen height reduction was kept as 50% for all specimens. Measurements were performed by using a digital vernier having an accuracy of 0.01 mm. Squared grids were machined on the surface by a special tool in the specimens midline having dimensions of 4 mm height and 4 mm width. Surface fractures were photographed using an Olympus digital camera.

RESULTS AND DISCUSSIONS

A sample of the stress-strain diagrams for the steel, Al alloy and brass specimens are given in Figures 2, 3 and 4 respectively. Different specimen geometry affected the slope of the curves and also affect the load values. Lubricated specimens gave less load values in all the materials tested. In all curves, large increase in stress was noticed first, followed by a uniform increase. This seems typical as the cylindrical specimens compression curve. Effect of the height to diameter ratio on the compression load for the different materials is illustrated in Figure 5. It is clear that the load increases as the ratio increases.

Typical strain/strain relationships for steel specimens having different geometries are presented in Figures 6-8. In general for cylindrical specimens, it was shown that the total axial and circumferential strains are proportional. The value of $\varepsilon_{\theta\ total}$ increases as $\varepsilon_{z\ total}$ increases. the lubricated specimens had higher values than these for dry ones. In some cases, however, this was not clear enough and the values were very close to each other in both cases. The values of $\varepsilon_{z\ total}$ were always larger than $\varepsilon_{\theta\ total}$ for all geometries, Figure 6 (a**)**. Values of the axial local strains ε_z local were proportional to these of the axial total strains ε_z total, and the local strain values are less than the total strain ones, Figure 6 (b). Values of the local circumferential strains $\varepsilon_{\theta local}$ were very close to the total circumferential strains $\varepsilon_{\theta\ total}$, and no clear trend was noticed, Figure 6(c).

For flanged specimens, (flange height is 50% of H_o), ε_θ total increase as $\varepsilon_{z\ total}$ increases and the axial strain values are always higher, Figure 7(a). Values of axial local strains $\varepsilon_{z\ \boldsymbol{local}}$ are inversely proportional to these of total strains $\varepsilon_{\boldsymbol{z\ total,}}$ provided that the total strains are always higher, Figure 7(b). When flange height was changed to a constant length of 2.75 mm (irrespective of the specimen height), the same above observations were present, Figures 7(d) and 7(e)**.** For the two cases of flanged specimens (concerning flange height), values of the local circumferential strains $\varepsilon_{\theta local}$ were very close to the total circumferential strains $\varepsilon_{\theta\ \boldsymbol{total}}$, and no clear trend was noticed, Figures 7(c) and 7(f)**.** The same remark was noticed for cylindrical specimens.

For tapered specimens having mid part height of 0.5 Ho and angle of the taper is 45^o, the same trends as flanged specimens were noticed, except that the values ε_z *local* are proportional to these of total strains ε_z total,. Figures 8 (a), (b), (c**).** When the cylindrical part height was fixed as 5.5 mm, and the small taper diameter is 0.5 D_o (meaning that the taper angle is not constant), the same above trends were noticed.

For a typical upsetting process, cracks appearing on the surface include external and longitudinal cracks, external shear cracks or external and mixing cracks [18-19]. External cracks appear at the specimen mid-height of side surface. For a crack to be

longitudinal or oblique depends on the degree of the constraint of specimen. Cracks of the ductile type were shown in steel specimens only, while the brittle type cracks were clear in the 4% Cu Al-base alloy and also in brass specimens. In cylindrical specimens, steel specimens did not show any crack up to 50% height reduction in both the dry and lubricated cases.

For flanged specimens, at constant flange height of 2.75 mm (1/8 of the original diameter), and at different H_o/D_o ratios, cracks of 90^o and 45^o appeared in the collar surface only at small H_o/D_o ratios and more severe in the dry condition. As the Ho/Do ratio increases, the cracks began in the collar and then extended to specimen body. For a Flange height of 50% of total specimen height with different H_o/D_o ratios, the same trend was observed. Steel tapered specimens with constant cylindrical mid part height of 5.5 mm (1/4 of the original height), showed 90^o cracks in the mid part at small Ho/Do ratios, extended to the specimen body for larger H_o/D_o ratios. As the mid part height is increased along with the increase in H_o/D_o ratio, 90^o and oblique cracks appeared and extended to the specimen body especially in larger Ho/Do ratios. Steel specimen cracks in the above cases are shown in Figure 9.

In Al alloy and brass cylindrical specimens, the fractures were similar. There were typical brittle fractures at about 55^o to the horizontal surface at small Ho/Do ratios. Final separation of the specimens was detected (for larger Ho/Do ratios). The specimens having $H_o/D_o = 1$. For the flanged specimens, at a constant flange height of 2.75 mm (1/8 of the original diameter), and at different H_o/D_o ratios, cracks of 45^o appeared in the coolar surface only at small H_o/D_o ratios and more severe in the dry condition. As the Ho/Do ratio increases, the cracks began in the collar and then extended to the specimen body. For a Flange height of 50% of the total specimen height with different Ho/Do ratios, the same trend did not show any change. For the tapered specimens, constant cylindrical midpart height of 5.5 mm (1/4 of the original height), 90^o cracks were observed in the cylindrical mid part at small Ho/Do ratios, extended to the tapered part for larger H_o/D_o ratios with the specimen separated to 2 pieces. As the mid part height is increased along with the increase in Ho/Do ratio, 90^o and oblique cracks appeared and extended to the tapered part especially in larger H_o/D_o ratios Aluminum alloy specimen cracks in the above cases are shown in Figure 10 while Brass specimen cracks in the above cases are shown in Figure 11.

CONCLUSIONS

1-Different specimen geometries affected the slope of the stress/strain curves and also affected the load values. The load increases as the H_o/D_o ratio increases for all geometries. The load value increases for dry specimens than lubricated ones. Different specimen geometry affected the slope of the curves to a little degree.

2- For cylindrical specimens, The values of ε_θ increases as ε_z increases. The values of ε_z are always larger for all geometries. The values of the local strains are also proportional to these of total strains. But always the local strain values are less than the total strain ones.

3- For flanged specimens, (flange height is 50% of Ho), $\varepsilon_{\theta\ total}$ increase as $\varepsilon_{z\ \boldsymbol{total}}$ increases and the axial strain values are always higher. Values of $\varepsilon_{z\ \boldsymbol{local}}$ are inversely proportional to these of $\varepsilon_{z\ \boldsymbol{total,}}$ provided that the total strains are always higher**.** When flange height have a length of 2.75 mm (irrespective of the specimen height), the same observations were present**.** Generally, $\varepsilon_{\theta\ local}$ were very close to $\varepsilon_{\theta\ total}$, and no clear trend

was noticed,. For tapered specimens having mid part height of 0.5 H_o and angle of the taper is 45°, the trends was the same as flanged specimens, except that the values $\varepsilon_{z\ local}$ are proportional to these of $\varepsilon_{z\ total}$,.

4- Cylindrical steel specimens did not show any crack up to 50% height reduction in both the dry and lubricated cases. Aluminum alloy and brass specimens showed typical brittle fractures at about 55° inclined to the horizontal surface at small Ho/Do ratios. Final separation of the specimens was detected. For the flanged specimens, at constant flange height of 2.75 mm different H_o/D_o ratios, steel and brass specimens showed cracks of 90° and 45° in the flange surface at small H_o/D_o ratios. For Aluminum alloy specimens, cracks of 45° appeared in the flange surface only at small H_o/D_o ratios and also more severe in the dry condition. For all materials. as the H_o/D_o ratio increases, the cracks began in the collar and then extended to the specimen body. For steel, Al alloy and brass tapered specimens, of a constant cylindrical mid part height of 5.5 mm, 90° cracks were observed in the mid part at small H_o/D_o ratios, extended to the specimen body for larger H_o/D_o ratios. As the mid part height is increased along with the increase in H_o/D_o ratio, 90° and oblique cracks appeared and extended to the specimens body in larger H_o/D_o ratios.

REFERENCES

[1] G. E. Deiter, in "Workability Testing Techniques", Metals Park,Ohio, ASM, (1983)

[2] D. V. Wilson , Influences of Metallurgical Structure on Formability", in Formability and Metallurgical Structure, Proc. Of a Symposium sponsored by TMS/AIME, Orlando, Florida, Oct. 5-9 1986, the Metall. Soc., (1987), pp3-32

[3] T. Erturk, W. L. Otto and H. A. Kuhn, "Anisotropy of Ductile Fracture in Hot Rolled Steel Plates- An Application of the Upset Test", Metall. Trans., volume 5 , Aug (1974), pp 1883-1886

[4] D. Vilotic and A. H. Shabaik, " Analysis of Upsetting With Profiling Dies", Journal of Engineering Materials and Technology, 107, Oct (1985), pp 261-264

[5] J. A. Schey and S. M Woodall, "Development of new Workability Testing Techniques", J. Mech. Working Tech., 2, (1979), pp 367-384

[6] A. M Sabroff, F. W. Bougler and H. J. Henning, Forging Materials and Practices, Reinhold, N. Y., (1968).

[7] H. Kudo and K . Aoi, "Effect of Compression Test Conditions Upon Fracturing of a Medium Carbon Steel- Study on Cold Forgeability Test: Part II", J. Japan Soc of the Tech op Plasticity, 8, (1967), pp 17-27

[8] S. Kobayashi, "Deformation Characteristics and Ductile Fracture of AISI 1040 Steel in Simple Upsetting of Solid Cylinders and Rings", J. Eng. For Ind., Trans ASME , May (1970) , pp 391-399

[9] H. A.Kukn, in Advances in Material Processing, Burke and Wells (Eds.),(1982)

[10] F. A. McClintock,"A Criterion for Ductile Fracture by the Groth of Holes"; J. Applied Mech., Trans. ASME, June (1968), pp 363-371

[11] Z. Marciniak and K. Kucznski, "Limit Strains in the Process of Stretch Forming Sheet Metals", Int. J. Mech. Sci., 9, (1967), 609-620.

[12] M. G. Cockroft and D. J. Latham, "Ductility and the Workability of Metals", J. Inst. Met., 96,(1968), pp 33-39

[13] A. Jenner , Y. Bai and B. Dodd, " A Thermoplastic Shear Instability Criterion Applied to Surface Cracking in Upsetting and Related Processes", J. Strain Anal. For
[14] M. Oyane, T. sato, K. Okimoto and S. Shima, "Criteria for Ductile Fracture and Their Applications", J. Mech, Wor. Tech,. 4, (1980), 65-81
[15] A. L. Hoffmanner, " The Use of Workability Test Results to Predict Processing Limits", Metal Forming Interrelation Between Theory and Practice, Proceedings of a Symposium, Cleveland , OH, , Oct 1970, Plenum Press, N. Y. 1971, pp 349-391
[16] V. Vujovic and A. H. Shabaik, "A New Workability Criterion For Ductile Metals", J. Eng. Mat and Tech, 108 , July (1986), 245-249
[17] E. Erman, H. A. Kuhn and G. Fitzsimons, "Novel Test Specimens for Workability Testing", Compression Testing of homogeneous Materials and Composites, ASTM special technical paper no. 808 , American Society for Testing and Materials, , R. Chait and R. Papirno (eds.) (1983), pp 279-290
[18] Tool and Manufacturing Engineers Handbook, TMEH, vol. 2 Forming, Charles Wick and Raymond F. Veilleux (editors), 4 th edition, Society for Mechanical Engineers, MI, (1984
[19] Metals Handbook, Vol. 14 Forming and Forging, ASM, Metals Park, OH, 9 th edition, (1988)

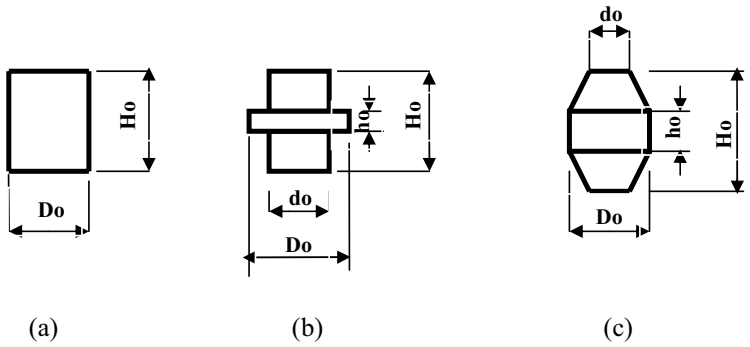

Figure 1: Specimen dimensions, 0.75, 1, 1.25 and 1.5 0.5
(a) Cylindrical specimens: Ho/Do ratios,
(b) Flanged specimens: ho/Do ratios of 0.25, 0.375, 0.5, 0.75 and 0.875and d_o/D_o ratios of 0.625, 0.75 and 0.875,
(c) Tapered specimens: ho/Do ratios of 0.25, 0.375, and 0.5, 0.75 and d_o/D_o ratios of 25, 0.375, 0.5, 0.75, 0.625 and 0.875.

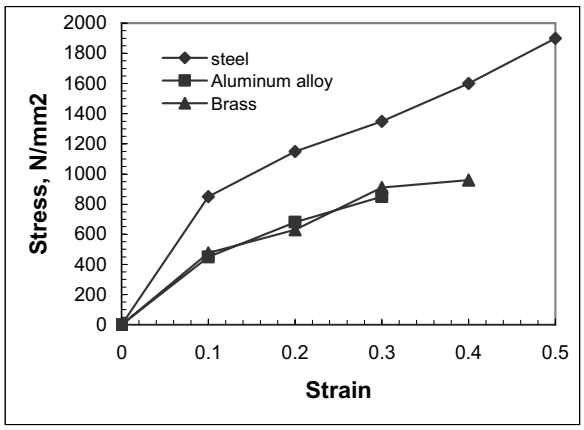

Figure 2: Stress-strain curves for cylindrical specimens, Ho/Do = 1.25

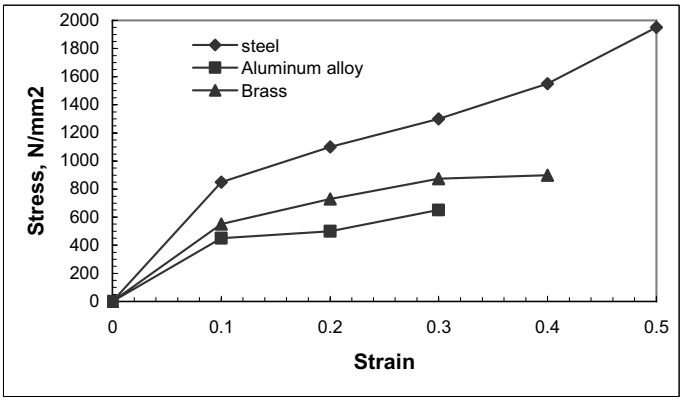

Figure 3: Stress-strain curves for flanged specimens, $H_o/D_o = 1.25$

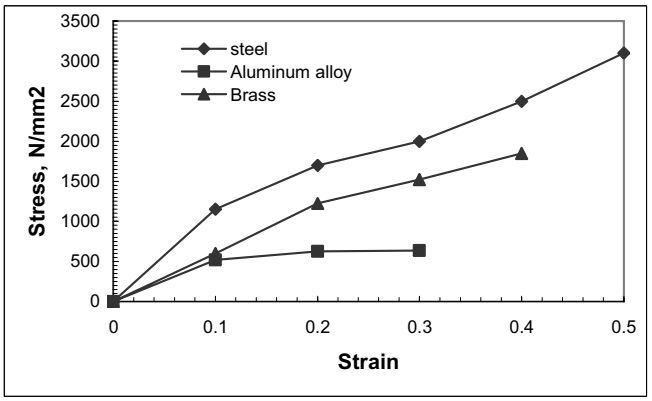

Figure 4: Stress-strain curves for tapered specimens, $H_o/D_o = 1.25$

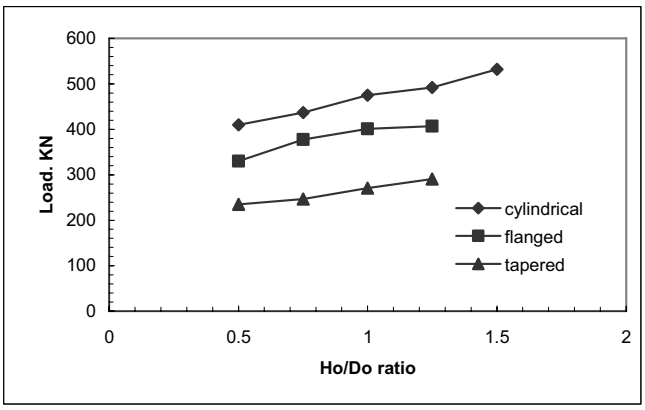

Figure 5: Effect of Ho/Do ratio on the compression load

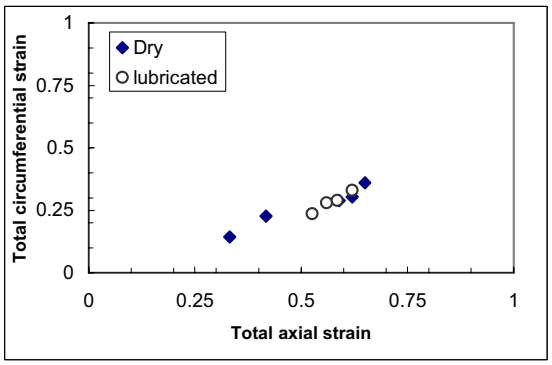

Figure 6 a: Total axial vs. circumferential strain for cylindrical steel specimens.

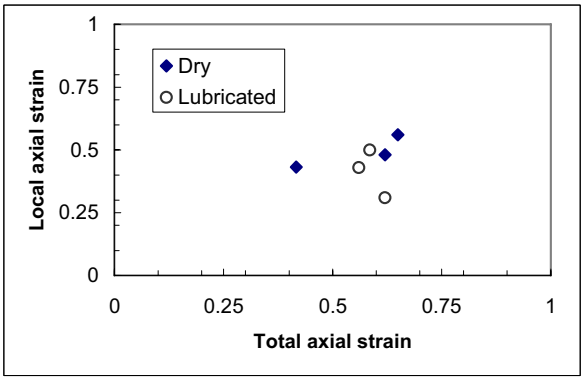

Figure 6b: Total axial vs. local axial strain for cylindrical steel specimens.

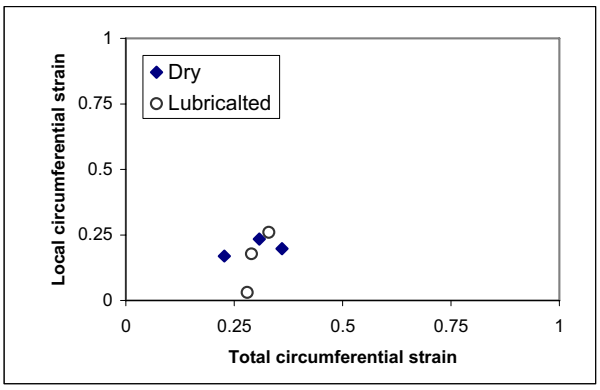

Figure 6c: Total circumferential vs. local circumferential strain values for cylindrical steel specimens.

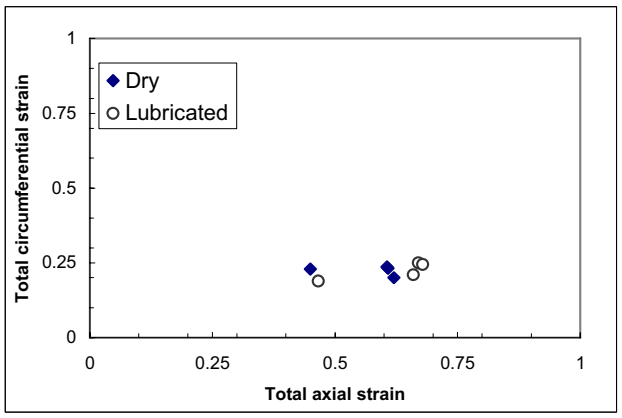

Figure 7a: Total axial vs. Total circumferential strain values for Flanged steel specimens.(Flange height = 0.5 of H_o)

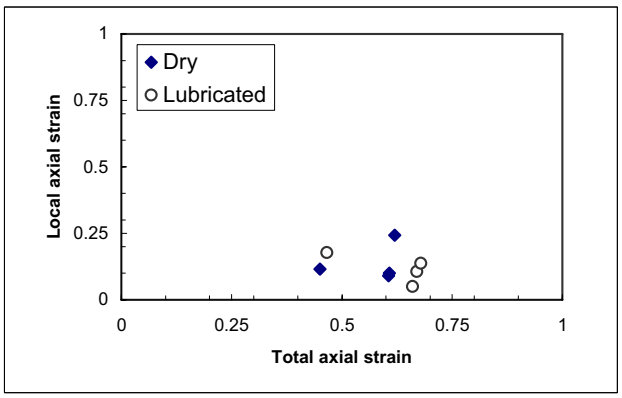

Figure 7b: Total vs. local axial strains for flanged steel specimens (Flange height = 0.5 H_o)

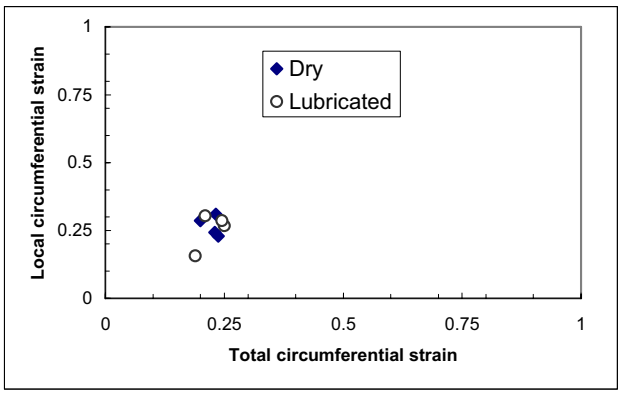

Figure 7c: Total vs. local circumferential strains, flanged steel specimens, Flange height 0.5 H_o)

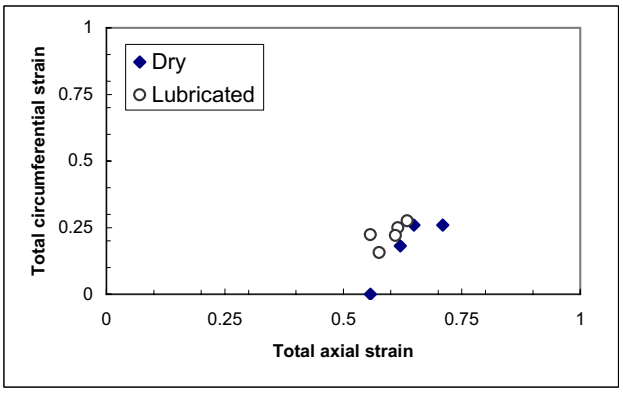

Figure 7d: Total axial vs. total circumferential strain values for Flanged steel specimens (Flange height = 2.75 mm = 1/8 of D_o) of H_o)

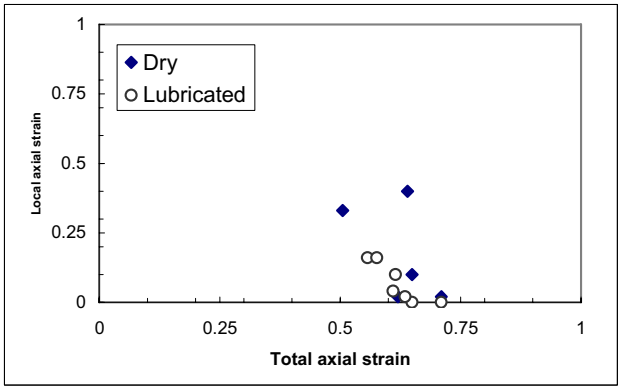

Figure 7e: Total axial vs. total circumferential strain values for Flanged steel specimens.(Flange height = 2.75 mm = 1/8 of D_o) of H_o)

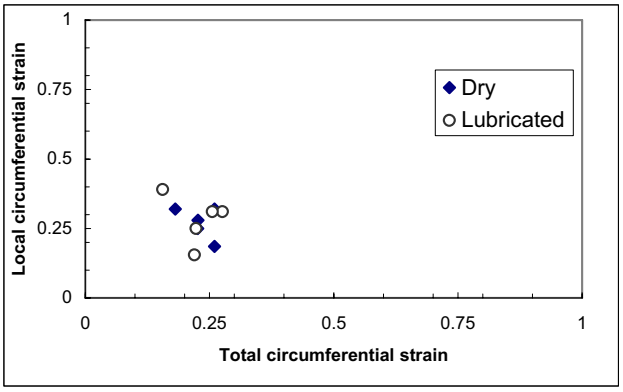

Figure 7f: Total vs. local circumferential strains for Flanged steel specimens.(Flange height = 2.75 mm = 1/8 of D_o) of H_o)

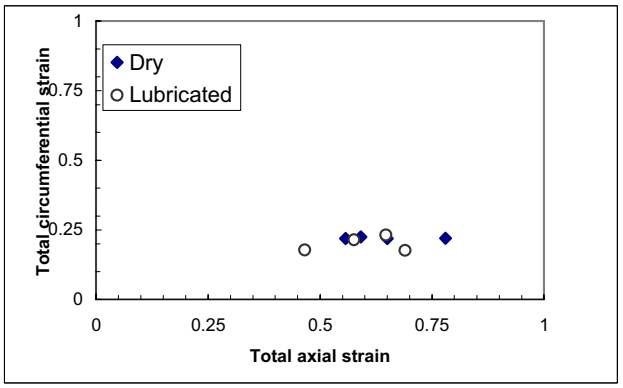

Figure 8a: Total axial vs. total circumferential strain values for tapered steel specimens, mid part height= 0.5 of Ho and taper angle is 45 degrees

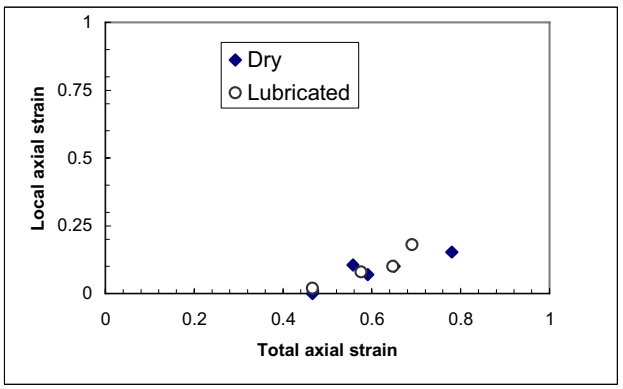

Figure 8b: Total vs. local axial strain values for tapered steel specimens, mid part height 0.5 of Ho and taper angle is 45 degrees

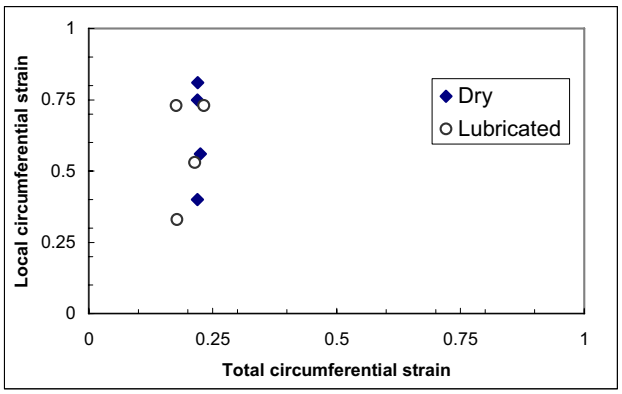

Figure 8c: Total vs. local circumferential strain values for tapered steel specimens, mid part height 0.5 of Ho and taper angle is 45 degrees

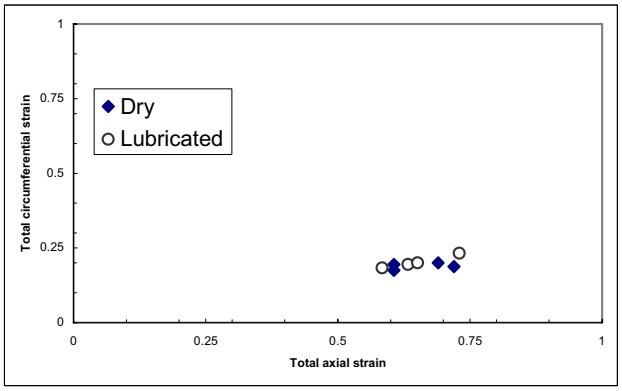

Figure 8d: Total axial vs total circumferential strain values for tapered steel specimens, mid part height = 0.25 of Do and small taper diameter = 0.5 D_o (taper angle is different)

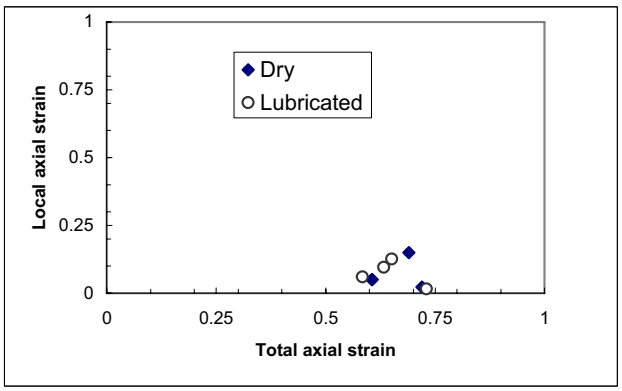

Figure 8e: Total axial vs local axial strain values for tapered steel specimens, mid part height = 0.25 of D_o and small taper diameter = 0.5 D_o (taper angle is different)

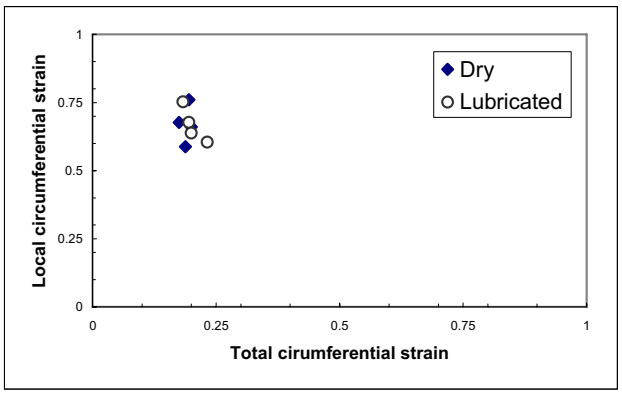

Figure 8f: Total circumferential vs. local circumferential strain values for tapered steel specimens, mid part height = 0.25 of Do and small taper diameter = 0.5 Do (taper angle is different)

(a)

(b)

(c)

(d)

(e)

Figure 9: Fractures on the surfaces of compressed steel specimens
a) Flanged, H_o/d_o 0.75, flange height 0.125 of D_o
b) Flanged, H_o/d_o 1.0, flange height 0.5 of Do
c) Tapered, H_o/D_o 0.5, mid part height 0.25 of D_o
d) Tapered, H_o/D_o 1.0, mid part height 0.25 of D_o
e) Tapered, H_o/D_o 0.75, mid part height 0.5 of D_o

(a) (b)

(c) (d)

(e) (f)

Figure 10: Fractures on the surfaces of compressed Al-based alloy specimens
a) Cylindrical, H_o/d_o 0.5,
b) Cylindrical, H_o/d_o 1.25
c) Cylindrical, H_o/d_o 1.25,
d) Flanged, H_o/D_o 1.25, flange height 0.125 of D_o
e) Tapered, H_o/D_o 1.25, mid part height 0.25 of D_o
f) Tapered, H_o/D_o 1.25, mid part height 0.5 of D_o

(a)

(b)

(c)

(d)

(e)

(f)

Figure 11: Fractures on the surfaces of compressed brass specimens
a) Cylindrical, H_o/d_o 1,
b) Cylindrical, H_o/d_o 1.5,
c) Flanged, , H_o/d_o 0.75, flange height 0.125 of D_o,
d) Flanged, H_o/D_o 1, flange height 0.5 of D_o,
e) Tapered, H_o/D_o 0.5, mid part height 0.25 of D_o,
f) Tapered, H_o/D_o 1, mid part height 0.5 of D_o